

# Decadal variability of Subtropical Mode Water subduction and its impact on biogeochemistry

Eitarou Oka<sup>1</sup> · Bo Qiu<sup>2</sup> · Yusuke Takatani<sup>3,4</sup> · Kazutaka Enyo<sup>3</sup> · Daisuke Sasano<sup>3,4</sup> · Naohiro Kosugi<sup>4</sup> · Masao Ishii<sup>3,4</sup> · Toshiya Nakano<sup>3,4</sup> · Toshio Suga<sup>5,6</sup>

Received: 20 January 2015 / Revised: 14 May 2015 / Accepted: 15 May 2015 / Published online: 4 June 2015  
© The Oceanographic Society of Japan and Springer Japan 2015

**Abstract** Temperature and salinity data from Argo profiling floats during 2005–2014 were analyzed to examine the decadal variability of the North Pacific Subtropical Mode Water (STMW) in relation to that of the Kuroshio Extension (KE) system. The formation volume of STMW in the southern recirculation gyre of KE in the cooling season was larger during the stable KE period after 2010 than the unstable KE period of 2006–2009 by 50 %. As a result, the volume and spatial extent of STMW increased (decreased) in the formation region during the stable (unstable) KE period, as well as in the southern, downstream region with a time lag of 1–2 years. The decadal expansion and contraction of STMW were also detected by shipboard observations conducted routinely in the most downstream region near the western boundary, in terms of not only physical, but also biogeochemical parameters. After 2010, enhanced subduction of STMW consistently increased dissolved oxygen, pH, and aragonite saturation

state and decreased potential vorticity, apparent oxygen utilization, nitrate, and dissolved inorganic carbon, among which changes of dissolved inorganic carbon, pH, and aragonite saturation state were against their long-term trends. These results indicate a new mechanism consisting of westward sea surface height anomaly propagation, the KE state transition, and the STMW formation and subduction, by which the climate variability affects physical and biogeochemical structures in the ocean's interior and potentially impacts the surface ocean acidification trend and biological production.

**Keywords** North Pacific Subtropical Mode Water · Subduction · Decadal variability · Kuroshio Extension · Biogeochemistry

## 1 Introduction

One of the most striking features revealed by the satellite altimeter sea surface height data during the past 22 years is the decadal variability of the Kuroshio Extension (KE) jet and its associated eddy field (Qiu and Chen 2005; Qiu et al. 2007, 2014; Figs. 1, 2) in association with the Pacific Decadal Oscillation (PDO; Mantua et al. 1997). When the PDO index is positive (negative), namely when the Aleutian Low is stronger (weaker), negative (positive) sea surface height and permanent pycnocline depth anomalies are generated in the central North Pacific, and then propagate westward at the speed of first-mode baroclinic Rossby waves. When the anomalies reach the area east of Japan after 3–4 years, KE turns into an unstable (stable) state, in which it takes a southerly (northerly) position and is accompanied by a weakened (strengthened) southern recirculation gyre and high (low) regional eddy activity.

✉ Eitarou Oka  
eoka@aori.u-tokyo.ac.jp

<sup>1</sup> Atmosphere and Ocean Research Institute, The University of Tokyo, Kashiwa 277-8564, Japan

<sup>2</sup> Department of Oceanography, University of Hawaii at Manoa, Honolulu, HI 96822, USA

<sup>3</sup> Global Environment and Marine Department, Japan Meteorological Agency, Tokyo 100-8122, Japan

<sup>4</sup> Oceanography and Geochemistry Research Department, Meteorological Research Institute, Tsukuba 305-0052, Japan

<sup>5</sup> Department of Geophysics, Graduate School of Science, Tohoku University, Sendai 980-8578, Japan

<sup>6</sup> Research and Development Center for Global Change, Japan Agency for Marine-Earth Science and Technology, Yokosuka 237-0061, Japan

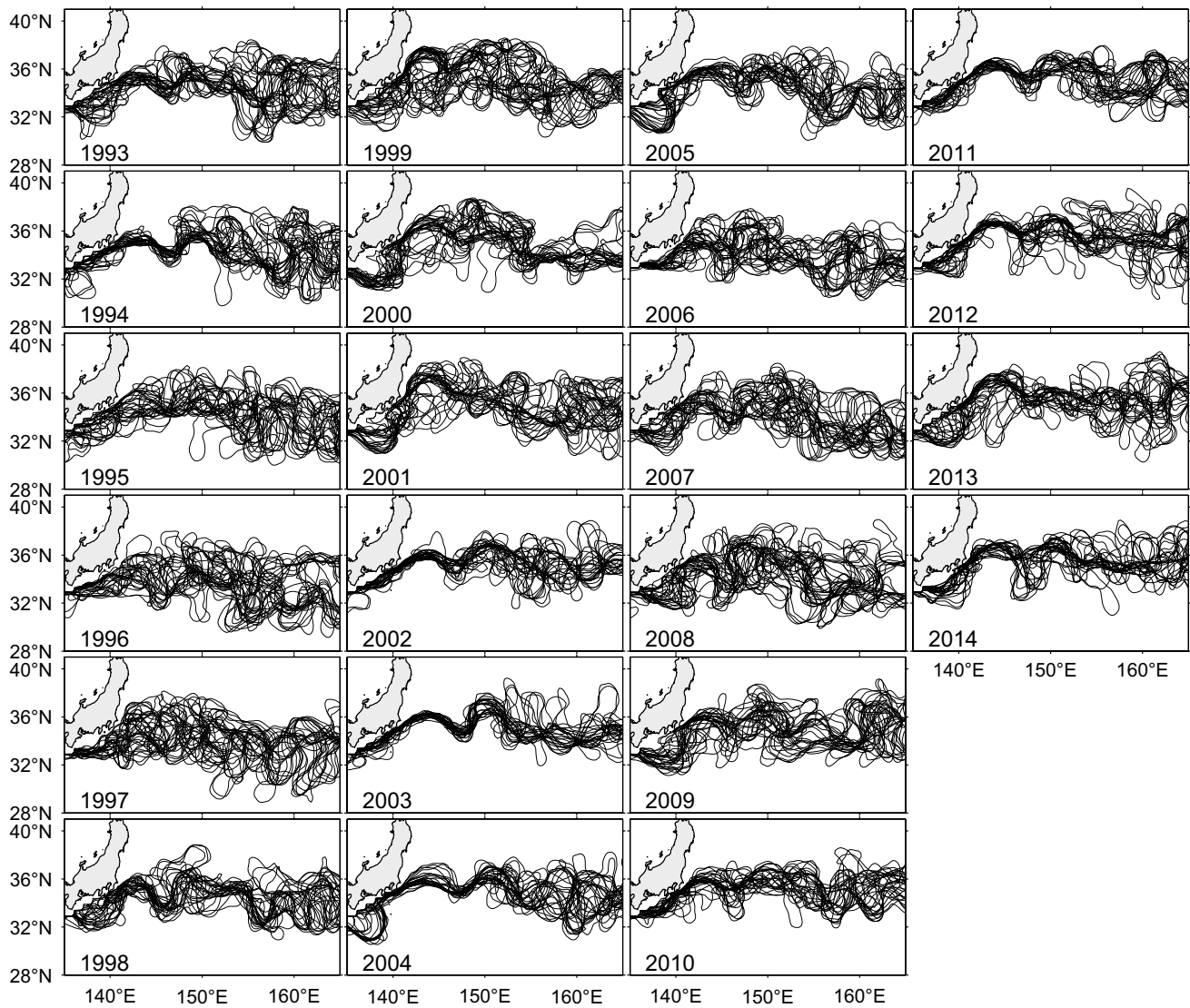


**Fig. 1** Yearly paths of the Kuroshio and KE plotted every 14 days using satellite altimeter sea surface height data, as in Qiu et al. (2014). KE was in a stable state in 1993–1994, 2002–2005, and 2010–, and in an unstable state in 1995–2001 and 2006–2009

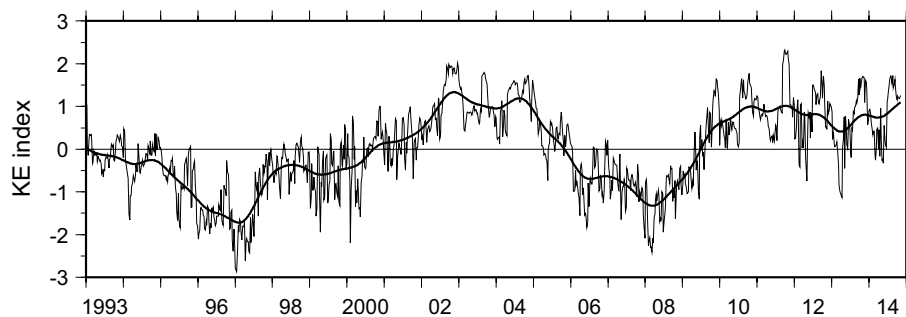


**Fig. 2** Time series of the KE index, defined by Qiu et al. (2014) as the average of four KE related parameters, normalized by their respective standard deviations. A positive (negative) KE index means

that KE has a stable (unstable) and northerly (southerly) path, an increased (decreased) surface transport, and a strengthened (weakened) southern recirculation gyre

This decadal variability of the KE system influences the formation, transportation, and modification of adjacent water masses, such as Subtropical Mode Water (STMW; Qiu and Chen 2006) and Central Mode Water (Oka et al. 2012), which account for the major portion of the upper and lower permanent pycnocline ventilation in the North Pacific subtropical gyre (Suga et al. 2008). An initial analysis of temperature profiles during 1993–2004 revealed that STMW formed in the southern recirculation gyre of KE was thicker (thinner) during the stable (unstable) KE period and that its thickness had little correlation with the oceanic heat loss to the atmosphere during the previous fall–winter (Qiu and Chen 2006). These findings were confirmed by subsequent studies with more recent observations (Miyazawa et al. 2009; Sugimoto and Hanawa 2010). The decadal STMW formation variability was attributed to water exchange across KE through the detachment of nonlinear mesoscale eddies (Qiu and Chen 2006); during the unstable KE period, more cyclonic eddies are detached from KE to the southern recirculation gyre and decay there (Sasaki and Minobe 2015), supplying water with relatively high potential vorticity north of KE to hinder the formation of deep winter mixed layers. Shallower permanent pycnocline and stronger background stratification during the unstable period also likely inhibit the formation of thick STMW (Sugimoto and Hanawa 2010).

Given the evident decadal STMW variability in its formation region, it is natural to ask how the KE variability influences the entire STMW distribution in the western part of the North Pacific subtropical gyre, whose variability is important not only physically (e.g., Sugimoto and Hanawa 2005; Xie et al. 2011; Kobashi and Kubokawa 2012; Kobashi et al. 2013), but also biogeochemically (e.g., Bates et al. 2002; Palter et al. 2005; Kr meur et al. 2009). After forming as deep mixed layers in the recirculation gyre north of 28°N in late winter (Oka and Suga 2003), STMW is advected southward across the mixed layer depth front at 28°N and is thereby subducted to the permanent pycnocline (Oka 2009; Oka et al. 2011), due partly to mesoscale eddy activities (Rainville et al. 2007; Nishikawa et al. 2010; Xu et al. 2014). Vigorous STMW formation during the stable KE period is likely to increase the entire STMW volume, while higher eddy activity during the unstable KE period might enhance the eddy subduction of STMW and increase its volume in the southern region (Oka and Qiu 2012).

The entire STMW distribution region has been monitored by a sufficient number of Argo profiling floats (Roemmich et al. 2001) since around 2005, thanks to intensive and continuous float deployment by various countries. The collected temperature and salinity data have clarified detailed seasonal and interannual variability of STMW and their relation to mesoscale eddies (Oka and Qiu 2012, and references therein), and have greatly improved our

understanding of STMW from the pre-Argo era when only climatological data and limited repeat hydrographic sections were available (e.g., Suga et al. 1989; Suga and Hanawa 1990, 1995a, b). Now that float data with dense spatial coverage have been accumulated for 10 years, it is worth exploring decadal variability of STMW in its entire distribution region. In this paper, we analyze the Argo float data during 2005–2014 to investigate the decadal STMW variability and its relation to the decadal KE variability. We also examine how the decadal STMW variability affects the physical and biogeochemical structures in the downstream, western boundary regions, based on long-term shipboard observation data.

In the past 10 years, KE was in a stable state from 2002 through 2005, switched to an unstable state in 2006–2009, and returned to the stable state in 2010 (Figs. 1, 2). The analysis period of 2005–2014 includes both the stable and unstable KE periods of nearly equal time lengths and is, therefore, well suited to examine the relationship between the decadal variability of STMW and that of KE.

## 2 Data and method

Temperature and salinity data from Argo profiling floats in the North Pacific from December 2004 through December 2014 were downloaded from the ftp site of the Argo Global Data Assembly Center (<ftp://usgodae.org/pub/outgoing/argo>, <ftp://ftp.ifremer.fr/ifremer/argo>) and edited as outlined in Oka et al. (2007). After discarding profiles shallower than 500 dbar and those in marginal seas, we vertically interpolated each profile onto a 1-dbar grid using the Akima spline (Akima 1970), and calculated potential temperature ( $\theta$ ),  $\sigma_\theta$ , and  $Q$ . Here, potential vorticity  $Q$  is defined as  $Q = gf \partial\sigma_\theta/\partial p$ , neglecting relative vorticity (e.g., Talley 1988; Oka et al. 2011), where  $f$  is the Coriolis parameter,  $g$  the gravity acceleration, and  $p$  is pressure.

We followed our previous studies (Oka 2009; Oka et al. 2011) to define STMW as a layer where  $Q$  is lower than  $2.0 \times 10^{-10} \text{ m}^{-1} \text{ s}^{-1}$  and  $\theta$  at the  $Q$  minimum is between 16 and 19.5 °C, except for those existing only at depths less than 100 dbar (in order to exclude spring–fall mixed layers with a thickness of several tens of meters). After detecting STMW in each float profile using this definition, we mapped the STMW thickness for each month according to the following procedure. First, the thickness values from float profiles in each  $1^\circ \times 1^\circ$  grid box were averaged to obtain the representative value at the center of the grid box (hereafter called grid point). Then, the mapped thickness at each grid point was calculated as the average of representative values at grid points within a search radius of  $1^\circ$  from the target grid point, if two or more representative values existed within the search radius. If only one or

no representative value existed, the search radius increased by 1°, up to a maximum of 5°, until we obtained two or more representative values. In such cases, the representative values were averaged using a weight function of  $d^{-2}$ , where  $d$  is the distance in degrees from each grid point to the target grid point. This interpolation procedure is similar to those used for the HydroBase climatology (Lozier et al. 1995; Macdonald et al. 2001; Suga et al. 2004) and was adopted to preserve the water mass structure in the KE frontal region as much as possible.

We used temperature and salinity data measured with a conductivity–temperature–depth profiler (CTD) in 32 cruises during 2005–2014 and dissolved O<sub>2</sub> data measured with a RINKO rapid-response sensor (JFE Advantech, Co.; Uchida et al. 2008) and calibrated with the data from discrete samples in 12 cruises after spring 2010 at the OK line. The data at 13 offshore CTD stations with the water depth exceeding 2000 m were analyzed. We also used temperature, salinity, and biogeochemical data collected with a CTD-carousel multi-sampler system in 45 cruises during 2002–2013 at a station at 25°N in the 137°E repeat hydrographic section. These observations were conducted routinely two to four times a year by R/V Chofu-maru, R/V Keifu-maru, and R/V Ryofu-maru of the Japan Meteorological Agency (JMA), and the collected data are publicly available through the JMA web site ([http://www.data.jma.go.jp/gmd/kaiyou/db/vessel\\_obs/data-report/html/ship/ship\\_e.php](http://www.data.jma.go.jp/gmd/kaiyou/db/vessel_obs/data-report/html/ship/ship_e.php)). Quality-controlled datasets including dissolved inorganic carbon (DIC) data are also available in the Pacific Ocean Interior Carbon Database (<http://cdiac.ornl.gov/oceans/PACIFICA/>). Methods for the measurements of dissolved O<sub>2</sub> and DIC were also explained in our previous studies (Ishii et al. 2011; Takatani et al. 2012).

### 3 Decadal variability of Subtropical Mode Water

STMW thickness in its formation region between the Kuroshio/KE and 28°N in late winter exhibited a significant decadal variation in relation to that of KE (Fig. 3). In 2005, STMW thicker than 300 dbar was formed at 142–156°E and 165–168°E, with a maximum thickness >400 dbar. In the following 4 years (2006–2009) of the unstable KE, the STMW thickness gradually decreased, as demonstrated by a recent study (Rainville et al. 2014), and its maximum fell down to 300 dbar in 2009. After the KE returned to the stable state in 2010, the STMW thickness gradually increased, and its values in 2014 returned to those observed in 2005. Thus, the thickness increased (decreased) during the stable (unstable) KE period, rather than being large (small) as described in the earlier studies (Qiu and Chen 2006; Miyazawa et al. 2009; Sugimoto and Hanawa 2010).

Late winter mixed layer depth distributions exhibit mixed layers deeper than 150 dbar only north of 28°N (Fig. 4), indicating that STMW observed south of 28°N in late winter was formed in the formation region in preceding winters and was then transported southward, as demonstrated in our previous studies (Oka 2009; Oka et al. 2011). This downstream STMW, which was subducted and advected southwestward to the western boundary (e.g., Suga and Hanawa 1995a; Oka 2009), also showed a decadal variation (Fig. 3). STMW thicker than 50 dbar broadly existed as far south as 18°N in 2005–2007, shrank considerably in 2010–2011, and recovered thereafter. (Its area south of 28°N was  $2.7 \times 10^{12} \text{ m}^2$  in 2005 and 2006, reduced to a minimum of  $0.8 \times 10^{12} \text{ m}^2$  in 2011, and returned to  $2.3 \times 10^{12} \text{ m}^2$  in 2014.) This corresponds to the STMW thickness variability in the formation region with a lag of about 1 year.

As the season progressed each year, STMW was gradually eroded, and concurrently, thick STMW formed in the formation region shifted southward (Fig. 5). In fall, the central latitude of the thick STMW shifted southward to about 28°N (Fig. 6), which was the southern limit of the STMW formation region in late winter (Fig. 3). The STMW thickness in fall also fluctuated decadal (Fig. 6). STMW thicker than 100 dbar was distributed broadly between 135° and 177°E in 2005, reduced to almost zero until 2010, and recovered after 2011.

These temporal variations of STMW are well quantified by its volume (Fig. 7a), which was computed from the monthly thickness distributions such as Figs. 3, 5, and 6. The total STMW volume exhibited both a seasonal variation, maximum in late winter (February–April) and minimum in fall (October–December), and a clear decadal variation characterized by a decrease in 2005–2009 and an increase after 2010. Its annual averages in 2005 ( $0.77 \times 10^{15} \text{ m}^3$ ) and 2014 ( $0.81 \times 10^{15} \text{ m}^3$ ) were twice as much as that in 2009 ( $0.40 \times 10^{15} \text{ m}^3$ ). The STMW volume in the formation region north of 28°N showed a similar variation to that in the whole distribution region, while that in the downstream region south of 28°N fluctuated decadal with a small seasonal variation, reaching a maximum in 2005–2006 and a minimum in 2010. As mentioned above, the STMW volume in the downstream region lagged about 1 year behind that in the formation region, indicating that low-frequency STMW variation in the formation region was transmitted to the downstream region through advection.

The decadal variation of STMW volume reflected that of the formation volume, which was calculated for each year as the difference between the maximum volume in late winter and the minimum volume in the previous fall in the formation region north of 28°N. The formation volume averaged in 2010/11–2013/14 during the stable KE

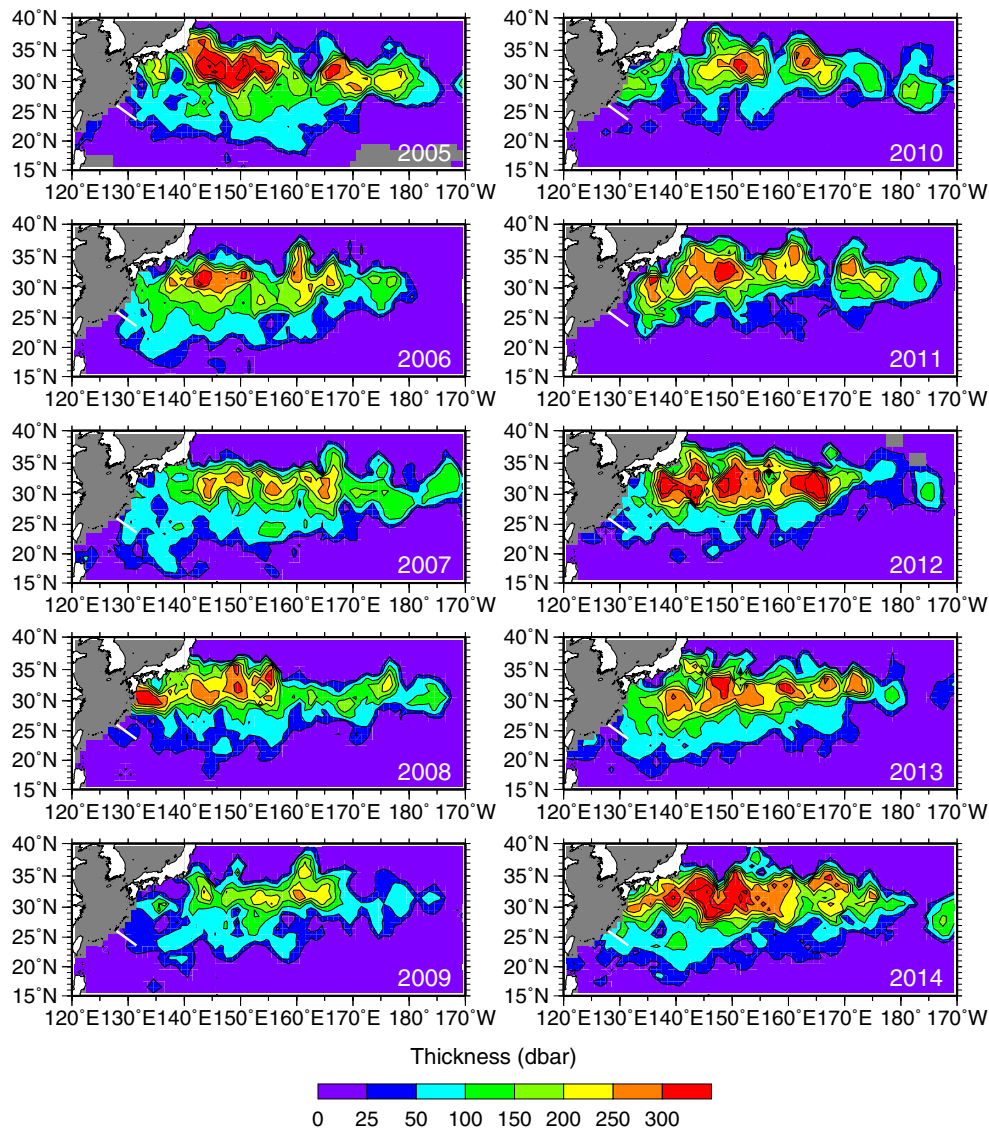


**Fig. 3** Distributions of STMW thickness in March, based on Argo float data. Contours are drawn at 25 dbar and every 50 dbar. *Thick white line* denotes the OK line

period was  $0.52 \times 10^{15} \text{ m}^3$ , and is larger by 53 % than that ( $0.34 \times 10^{15} \text{ m}^3$ ) averaged in 2006/07–2008/09 during the unstable KE period (Fig. 7b). As discussed in the previous studies (Qiu and Chen 2006; Sugimoto and Hanawa 2010), more vigorous water exchange across KE and stronger background stratification in the STMW formation region during the unstable KE period are believed to weaken the STMW formation. Smaller outcropping area due to the southerly KE position and to masking by cyclonic eddies (Rainville et al. 2007) during the same period are also expected to contribute to the smaller formation volume.

The erosion volume of STMW, calculated as the difference between the maximum volume in late winter and the minimum volume in the following fall in the formation

region, was also larger in 2010–2014 during the stable KE period ( $0.45 \times 10^{15} \text{ m}^3$  on average) than in 2006–2009 during the unstable KE period ( $0.39 \times 10^{15} \text{ m}^3$ ) by 15 %. Notice that the erosion volume during the stable (unstable) KE period was smaller (larger) than the formation volume during the same period by  $0.07$  ( $0.05$ )  $\times 10^{15} \text{ m}^3$ , resulting in that the STMW volume in the formation region increased (decreased) during the stable (unstable) KE period (Fig. 7a). The erosion volume consists mainly of volume dissipated in the formation region and that transported to the downstream region south of  $28^\circ\text{N}$ , the latter of which contributed to the lagged volume increase (decrease) in the downstream region during the stable (unstable) KE period.

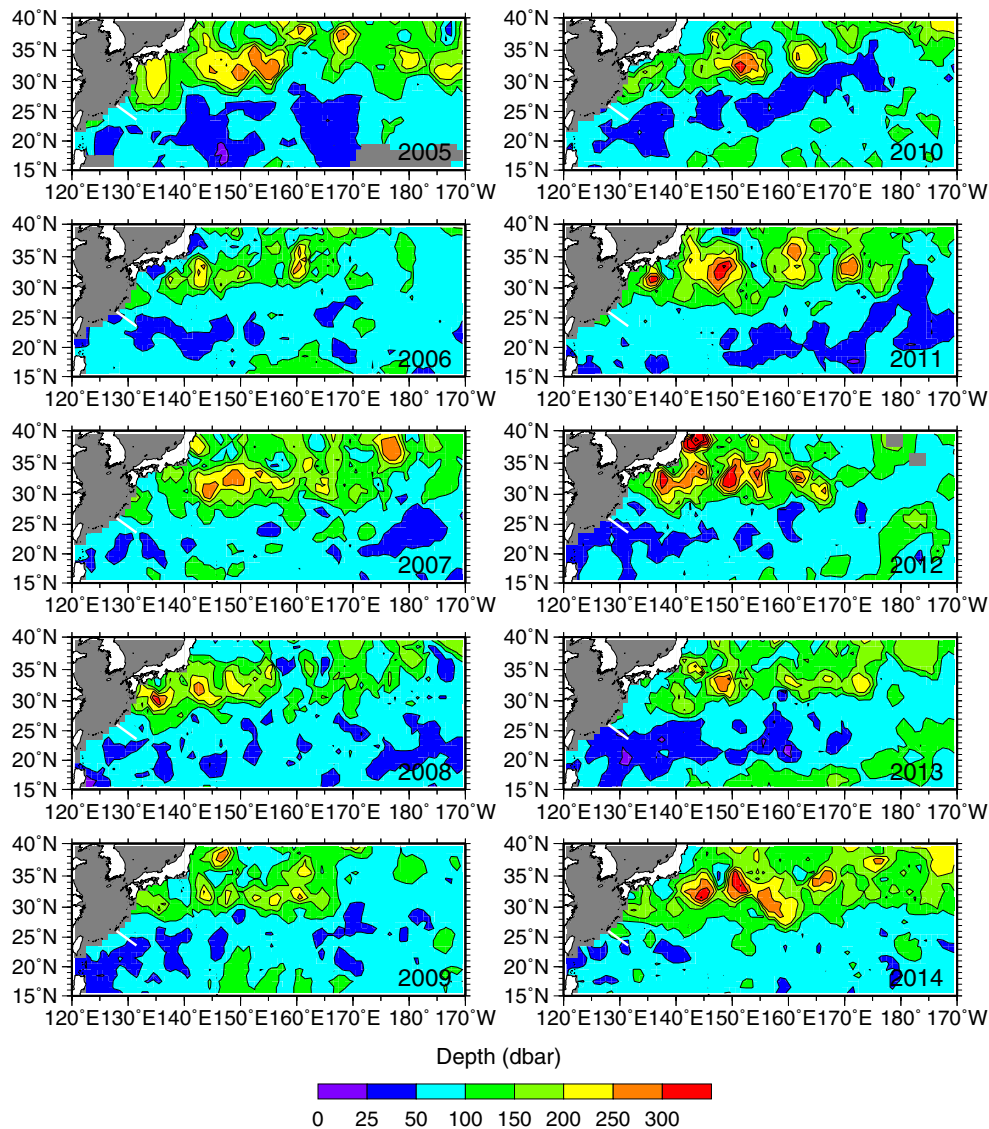


**Fig. 4** Distributions of mixed layer depth in March, otherwise following Fig. 3. Mixed layer depth, which is defined as the shallower value of the depth at which  $\sigma_\theta$  increases by  $0.125 \text{ kg m}^{-3}$  from 10-dbar depth and that at which  $\theta$  changes by  $0.5 \text{ }^\circ\text{C}$  from 10-dbar

depth (e.g., Levitus 1982; Suga et al. 2004), was computed for each float profile and then mapped using the same procedure as for STMW thickness

#### 4 Biogeochemical influence in the downstream region

Decadal variability of STMW formation and subduction was also detected in the most downstream region at the OK line just southeast of the Okinawa Island (thick white line in Figs. 3, 4, 5, and 6), where JMA has conducted shipboard observations routinely two to four times a year. The STMW area in the OK section (Fig. 7c) exhibited a decadal variation, being large in 2006–2007, small in 2010, and large in 2012–2014, with a shorter-term variation possibly related to meso-scale activities (e.g., Takikawa et al. 2005). This

decadal variation at the OK line seems to lag about 0.5 year behind that in the STMW downstream region and about 1.5 years behind that in its formation region (Fig. 7a).<sup>1</sup>

<sup>1</sup> The correlation between the STMW area in the OK section (Fig. 7c) and the STMW volume south of  $28^\circ\text{N}$  (Fig. 7a, blue line) is 0.5–0.6 with a time lag of 0–10 months and drops with a longer time lag. The correlation with low-frequency variation of the STMW volume north of  $28^\circ\text{N}$  (Fig. 7a, red line), which is obtained by subtracting its monthly average, has a peak of  $\sim 0.6$  at a time lag of 13–16 months.

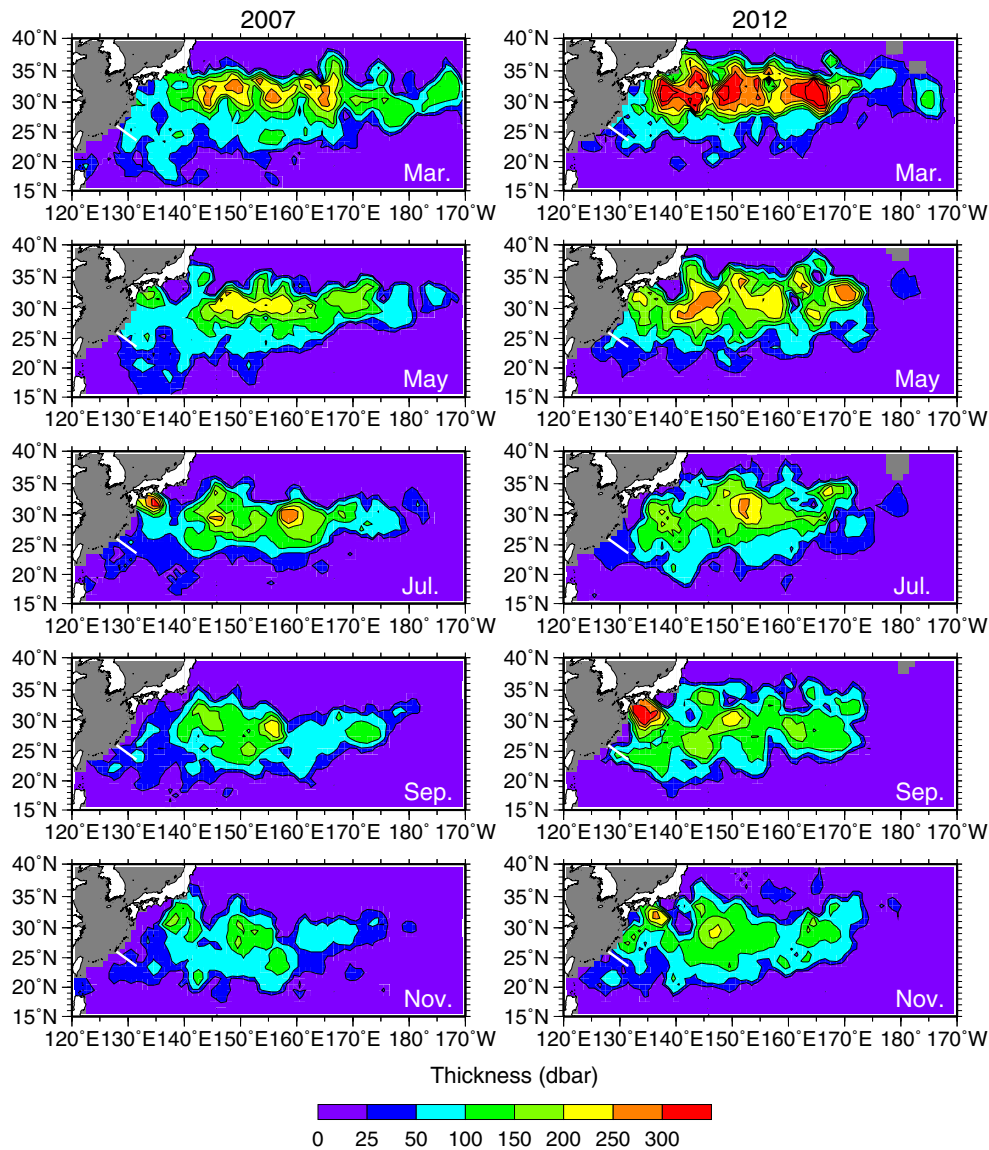


**Fig. 5** Seasonal evolution of STMW thickness in 2007 (*left*) and 2012 (*right*), otherwise following Fig. 3

In addition, concurrent sensor measurements of temperature, salinity, and dissolved oxygen ( $O_2$ ) available after spring 2010 at the OK line reveal not only a potential vorticity ( $Q$ ) decrease, but also a dissolved  $O_2$  increase and an apparent oxygen utilization (AOU) decrease on the isopycnals of  $\sigma_\theta = 24.8\text{--}25.4 \text{ kg m}^{-3}$  ( $\sigma_\theta$  is potential density), which correspond to the isotherms of  $16.5\text{--}19.4 \text{ }^\circ\text{C}$  in the STMW temperature range (Fig. 8). The increased advection of  $O_2$ -rich STMW during the stable KE period is thought to enhance the oxygen supply to the subsurface layer at the OK line. Such consistent and significant changes of  $Q$ , dissolved  $O_2$ , and AOU were limited to the STMW-related isopycnals (Fig. 9). At depths greater than  $\sigma_\theta = 25.4 \text{ kg m}^{-3}$ , the change rates dropped quickly. At depths less than  $24.8 \text{ kg m}^{-3}$ , dissolved  $O_2$  increased and

AOU decreased at similar rates to the STMW layer, but  $Q$  increased. It should be noted that the changes of  $Q$ , dissolved  $O_2$ , and AOU were observed not only on isopycnals corresponding to lighter STMW originating in the western part of the formation region south of Japan, but also on those corresponding to denser STMW formed in the eastern part of the formation region. In other words, the hydrographic structure at the OK line in the western boundary region reflected the decadal variation of STMW formation in its entire formation region that spreads zonally south of the Kuroshio and KE (Oka and Suga 2003; Oka 2009).

The downstream influence of STMW advection was further examined using the shipboard observation data at  $25^\circ\text{N}$  in the  $137^\circ\text{E}$  repeat hydrographic section of JMA, located about 500 km east/upstream of the OK line, where

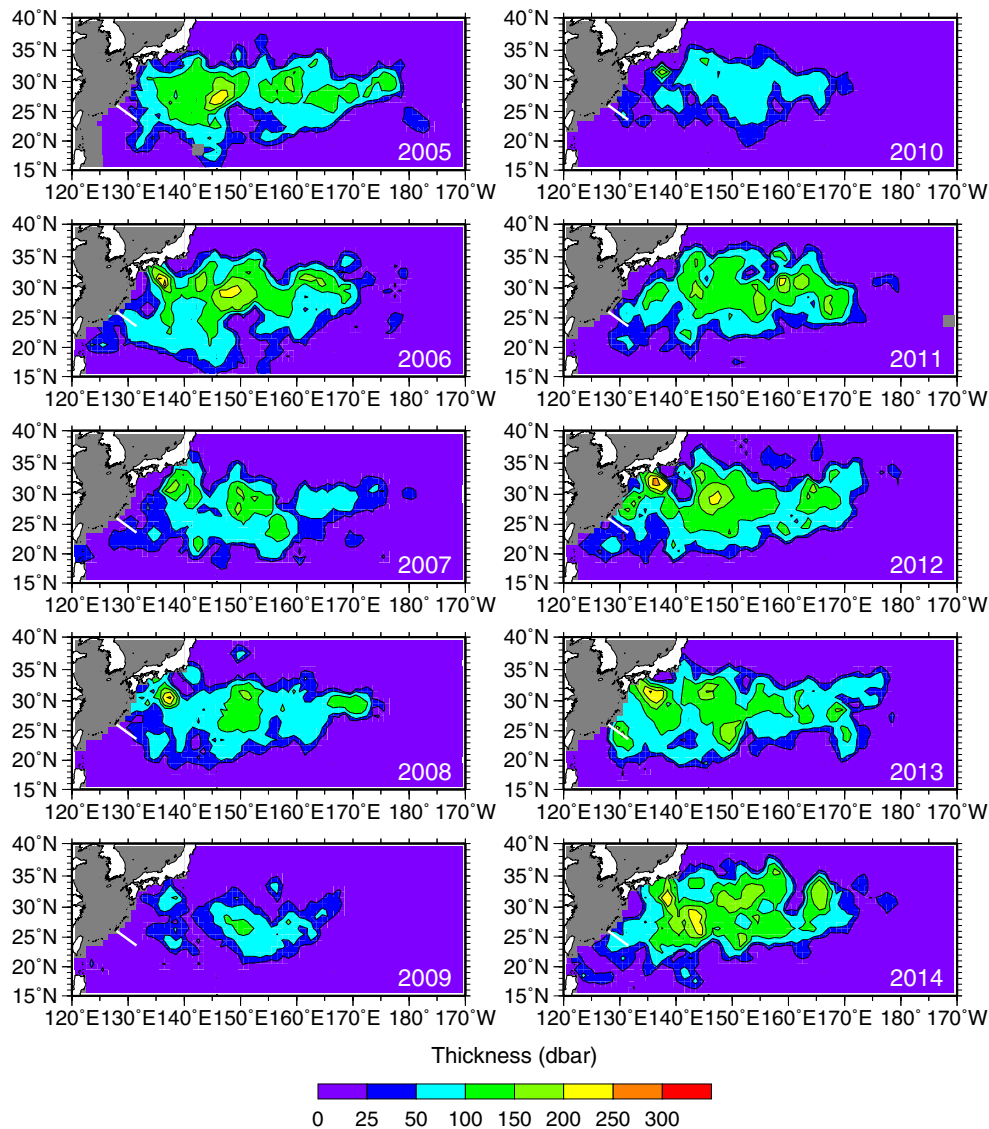


**Fig. 6** Distributions of STMW thickness in November, otherwise following Fig. 3

various biogeochemical parameters have been monitored (e.g., Ishii et al. 2001, 2011; Midorikawa et al. 2006; Takatani et al. 2012). Six biogeochemical parameters derived from discrete water samples taken at depths, specifically AOU, salinity-normalized dissolved inorganic carbon (nDIC), preformed nDIC, pH, aragonite saturation state index ( $\Omega_{\text{arag}}$ ), and nitrate ( $\text{NO}_3$ ) concentration, were interpolated onto the  $\sigma_\theta = 25.0 \text{ kg m}^{-3}$  isopycnal for the period of 2002–2013 (Fig. 10). In 2011–2013, we observed a remarkable AOU decrease due to the increased advection of more recently ventilated STMW, as in the OK line (Fig. 8c). An nDIC decrease was also observed, in spite of a steady increase in preformed nDIC throughout the observation period reflecting the increase of anthropogenic  $\text{CO}_2$  content. As a result of the nDIC decrease, pH and  $\Omega_{\text{arag}}$

increased in 2011–2013, in contrast to their long-term decreasing trends indicating ocean acidification.  $\text{NO}_3$  concentration decreased in the same period, which, together with the decreases of AOU and nDIC, is expected to reflect the reduction in the transformation of organic matters to inorganic form, i.e., remineralization, as a result of the increased STMW advection.

The influence of the STMW advection on the nutrient concentration in the downstream has also been suggested in the North Atlantic. At the Bermuda Atlantic Time Series station located south of the formation region of North Atlantic STMW, long-term measurements of physical and biogeochemical parameters revealed a positive correlation between  $Q$  and  $\text{NO}_3$  concentration in STMW (Palter et al. 2005). This relationship indicates that  $\text{NO}_3$  concentration



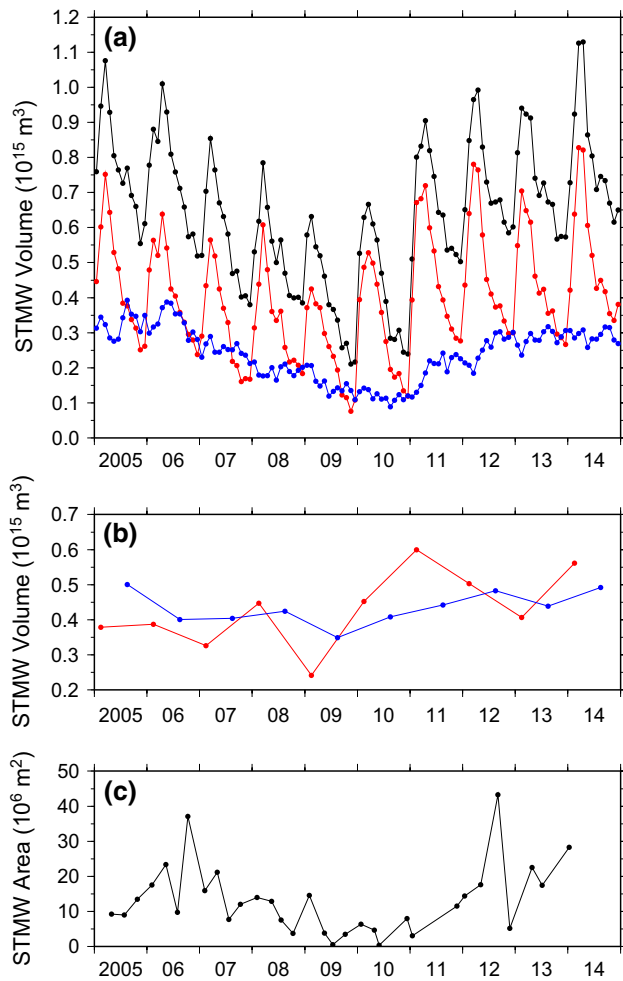


**Fig. 7** **a** Monthly time series of STMW volume at 15°–40°N (black line), 28°–40°N (red line), and 15°–28°N (blue line) between 120°E and 170°W, based on Argo float data. **b** Time series of formation volume (red line) and erosion volume (blue line) of STMW north of 28°N, between 120°E and 170°W, based on Argo float data. **c** Time series of STMW area in the vertical section of the OK line, based on shipboard observations

in the downstream region tends to be lower when a more recently ventilated STMW reaches the station. The downstream  $\text{NO}_3$  concentration fluctuation in the North Pacific STMW might have also partly originated in the STMW formation region, where  $\text{NO}_3$  concentration tends to be low (high) during the stable (unstable) KE period, probably due to the inactive (active) water exchange between the  $\text{NO}_3$ -depleted oligotrophic subtropical gyre and the eutrophic mixed water region across the KE (Kouketsu et al. 2015). Such a contribution from the STMW formation region potentially reinforces the concentration changes in the downstream through advection, and needs to be quantified in future studies.

The above changes of biogeochemical parameters at 25°N, 137°E were all consistent with one another and are

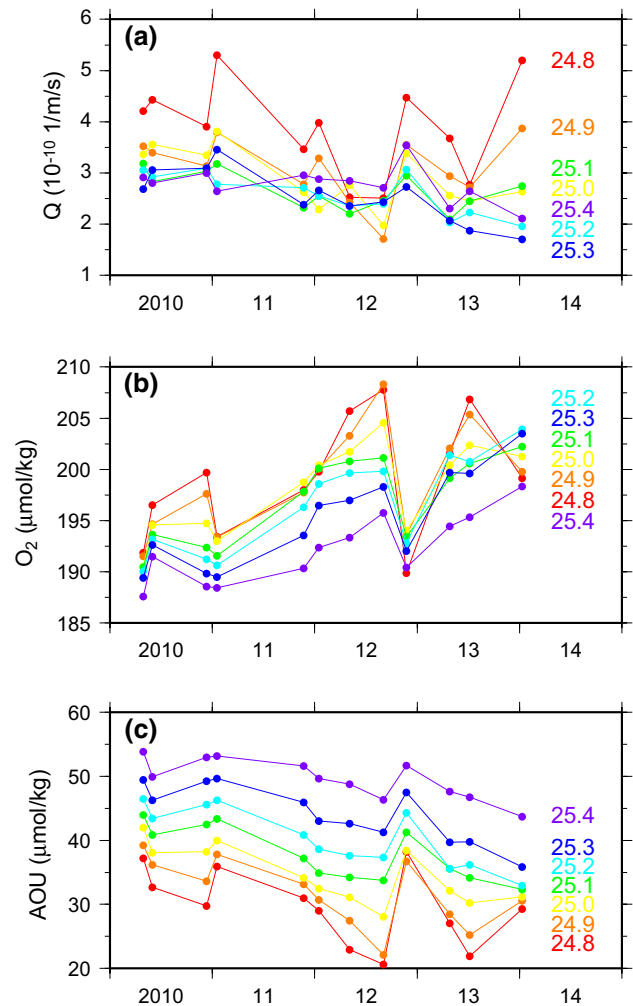


**Fig. 8** Time series of **a**  $Q$ , **b** dissolved  $\text{O}_2$ , and **c** AOU on the isopycnals of  $\sigma_\theta = 24.8\text{--}25.4 \text{ kg m}^{-3}$ , based on shipboard observations at the OK line

expected to reverse during the unstable KE period when the STMW advection weakens. In fact, AOU exhibited a slight decrease from mid-2003 to mid-2007 and a gradual increase from mid-2007 through 2010, lagging 1.5 years behind the stable KE period in 2002–2005 and the unstable KE period in 2006–2009. If it had been measured by a sensor with 1-dbar resolution, we might have obtained its clearer decadal variation. AOU changes in the coming unstable KE period should be verified by sensor measurements.

## 5 Discussion

The findings of the present and previous (Qiu and Chen 2005, 2006; Qiu et al. 2007, 2014) studies point to an integrated decadal climate-physical-biogeochemical variability

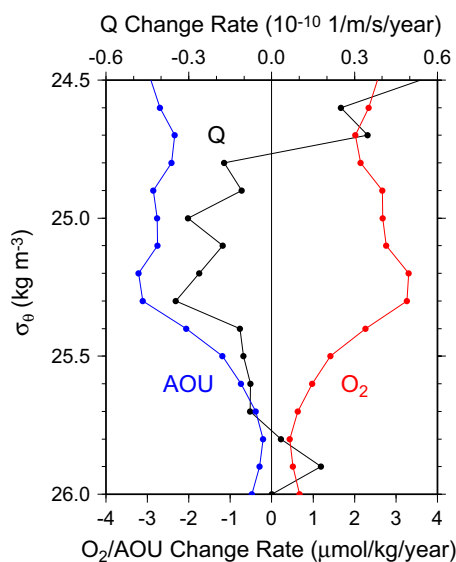


**Fig. 9** Change rates of  $Q$ , dissolved  $O_2$ , and AOU on the isopycnals of  $\sigma_\theta = 24.5\text{--}26.0 \text{ kg m}^{-3}$ , calculated from shipboard observation data at the OK line during 2010–2014 using the least squares method

across the North Pacific basin. Specifically, a strengthened (weakened) Aleutian Low in the positive (negative) PDO phase destabilizes (stabilizes) the KE system 3–4 years later, and the associated high (low) eddy activity modulates the mixed layer processes in the southern recirculation gyre on a decadal time scale, leading to the formation of thinner (thicker) STMW. As a result, the volume and extent of STMW decrease (increase) in the formation region during the unstable (stable) KE period, as well as in the southern, downstream region with a time lag of 1–2 years. In the latter region, weakened (intensified) advection of young,  $O_2$ -rich STMW increases (decreases)  $NO_3$  and nDIC and thereby decreases (increases) pH and  $\Omega_{\text{arag}}$ . To put it more plainly, it is the intensification (weakening) of the Aleutian Low that subsequently accelerates (slows down) acidification in the subsurface ocean near the Okinawa Island. The observed fluctuations in biogeochemical parameters are important not only for understanding the mechanism of subsurface biogeochemical variations but also for quantifying correctly the long-term trends of ocean acidification from records that only span for a decade or two (e.g., Dore et al. 2009; Midorikawa et al. 2010; Ishii et al. 2011).

The present results have broad implications. First, it is important to investigate how the observed biogeochemical variability in the subsurface affects the surface environment in the subtropical regions of the western North Pacific, particularly the region near the Okinawa Island known for its coral reefs. The increasing  $O_2$  trend at depths less than  $\sigma_\theta = 24.8 \text{ kg m}^{-3}$  (Fig. 9) might indicate that oxygen (and other substances) was supplied from

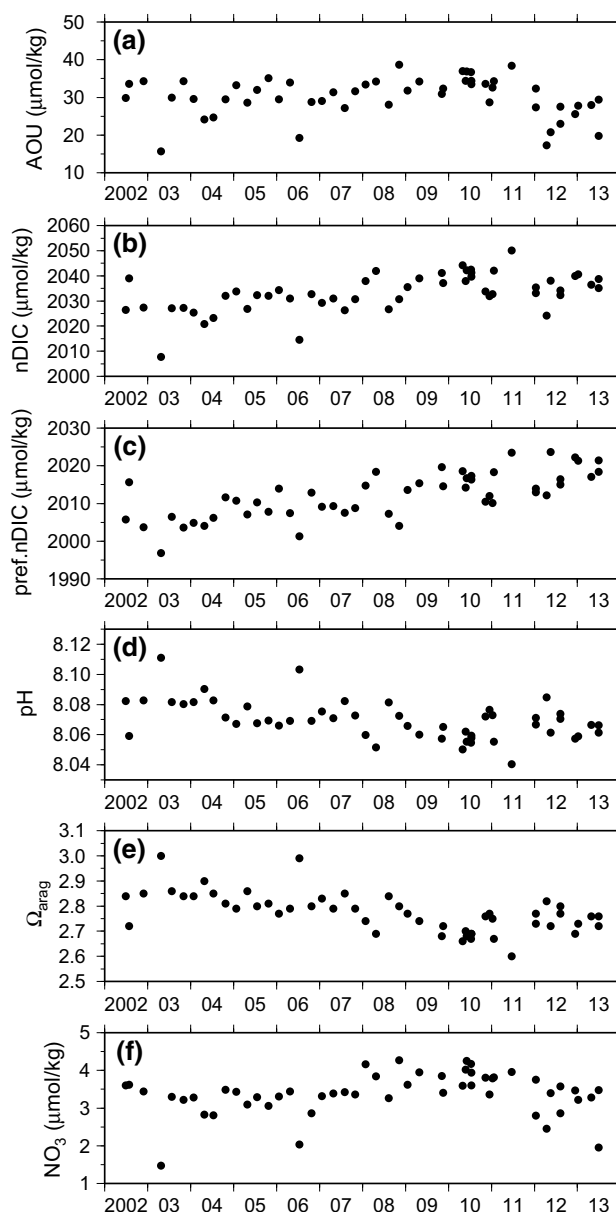


**Fig. 10** Time series of **a** AOU, **b** nDIC, **c** preformed nDIC, **d** pH, **e**  $\Omega_{\text{arag}}$ , and **f**  $NO_3$  concentration on the isopycnal of  $\sigma_\theta = 25.0 \text{ kg m}^{-3}$ , based on shipboard observations at  $25^\circ\text{N}$ ,  $137^\circ\text{E}$

the STMW layer to the shallower layers through diapycnal mixing. If the variability in  $NO_3$  concentration in the STMW layer is transmitted to the surface layer, it might have a notable impact on the primary production there. On the other hand, considering that the consumption of  $NO_3$  by production is associated with that of nDIC, the variability in the STMW subduction and the resultant changes in the upward  $NO_3$ /nDIC flux might not influence directly the rate of ocean acidification at the sea surface. Nevertheless, the formation and subduction of STMW play an important role in transporting anthropogenic  $CO_2$  from

the sea surface to the ocean interior in the subtropics, and its erosion by diapycnal mixing in the downstream region contributes to the reemergence of anthropogenic CO<sub>2</sub> to the sea surface. Secondly, the significant decadal variability of STMW is expected to be accompanied by that of thermal structure, which is reflected in the upper-ocean heat content in the western part of the subtropical gyre and possibly modulates the sea surface temperature through the generation of the Subtropical Countercurrent (Xie et al. 2011; Kobashi and Kubokawa 2012). Furthermore, the linkage between the climate and biogeochemical variability through the formation, subduction, and advection of STMW might be applicable to other mode waters in the world oceans (Hanawa and Talley 2001), whose formation regions are characterized by high air-to-sea CO<sub>2</sub> flux (Takahashi et al. 2009). It is worth emphasizing finally that the decadal oscillation across the North Pacific basin and its mechanism have been clarified thanks to the sustained observations by the satellites, the Argo float network, and the research vessels. Synthetic analyses of these data will further clarify decadal variations in the ocean interior and their impact on biogeochemical variations and changes.

**Acknowledgments** The authors are grateful to the captain, crew, and scientists of R/V *Chofu-maru*, R/V *Keifu-maru*, and R/V *Ryofu-maru* of JMA for their efforts in long-term observations. They also thank Kanako Sato and Kana Nakamoto for their assistance in preparing the Argo float data and Yosuke Iida, Atsushi Kojima, Tomoyuki Kitamura, participants at the 2014 HYARC symposium on air–sea interaction, and two anonymous reviewers for helpful comments on the manuscript. E.O. and T.S. acknowledge support by JSPS through Grant 21340133 and 25287118 and MEXT through 22106007. E.O. is also supported by MEXT through 25121502. B.Q. acknowledges support by NASA through Grant NNX13AE51G and NSF through OCE-0926594. D.S. acknowledges support by JSPS through 24241010. M.I. acknowledges support by MRI's key research fund C3 and MEXT through 24121003.

## References

- Akima H (1970) A new method of interpolation and smooth curve fitting based on local procedures. *J Assoc Comput Math* 17:589–602
- Bates NR, Pequignet AC, Johnson RJ, Gruber N (2002) A variable sink for atmospheric CO<sub>2</sub> in subtropical mode water of the North Atlantic Ocean. *Nature* 420:489–493
- Dore JE, Lukas R, Sadler DW, Church MJ, Karl DM (2009) Physical and biogeochemical modulation of ocean acidification in the central North Pacific. *Proc Natl Acad Sci USA* 106:12235–12240
- Hanawa K, Talley LD (2001) Mode waters. In: Church J et al (eds) *Ocean circulation and climate*. Academic Press, London, pp 373–386
- Ishii M, Inoue HY, Matsueda H, Saito S, Fushimi K, Nemoto K, Yano T, Nagai H, Midorikawa T (2001) Seasonal variation in total inorganic carbon and its controlling processes in surface waters of the western North Pacific subtropical gyre. *Mar Chem* 75:17–32
- Ishii M, Kosugi N, Sasano D, Saito S, Midorikawa T, Inoue HY (2011) Ocean acidification off the south coast of Japan: a result from time series observations of CO<sub>2</sub> parameters from 1994 to 2008. *J Geophys Res* 116:C06022. doi:10.1029/2010JC006831
- Kobashi F, Kubokawa A (2012) Review on North Pacific Subtropical Countercurrent and Subtropical Front: role of mode water in ocean circulation and climate. *J Oceanogr* 68:21–43
- Kobashi F, Hosoda S, Iwasaka N (2013) Decadal variations of the North Pacific Subtropical Mode Water and Subtropical Countercurrent. *Bull Coast Oceanogr* 50:119–129 (in Japanese with English abstract)
- Kouketsu S, Kaneko H, Okunishi T, Sasaoka K, Itoh S, Inoue R, Ueno H (2015) Mesoscale eddy effects on temporal variability of surface chlorophyll *a* in the Kuroshio Extension. *J Oceanogr* (in press)
- Krémeur AS, Lévy M, Aumont O, Reverdin G (2009) Impact of the subtropical mode water biogeochemical properties on primary production in the North Atlantic: new insights from an idealized model study. *J Geophys Res* 114:C07019. doi:10.1029/2008JC005161
- Levitus S (1982) *Climatological atlas of the world ocean*. NOAA professional paper 13. US Government Printing Office, Washington, DC, p 173
- Lozier SM, Owens WB, Curry RG (1995) The climatology of the North Atlantic. *Prog Oceanogr* 36:1–44
- Macdonald AM, Suga T, Curry RG (2001) An isopycnally averaged North Pacific climatology. *J Atmos Oceanic Technol* 18:394–420
- Mantua NJ, Hare SR, Zhang Y, Wallace JM, Francis RC (1997) A Pacific interdecadal climate oscillation with impacts on salmon production. *Bull Amer Meteor Soc* 78:1069–1079
- Midorikawa T, Ishii M, Nemoto K, Kamiya H, Nakadate A, Masuda S, Matsueda H, Nakano T, Inoue HY (2006) Interannual variability of winter oceanic CO<sub>2</sub> and air–sea CO<sub>2</sub> flux in the western North Pacific for 2 decades. *J Geophys Res* 111:C07S02. doi:10.1029/2005JC003095
- Midorikawa T, Ishii M, Saito S, Sasano D, Kosugi N, Motoi T, Kamiya H, Nakadate A, Nemoto K, Inoue HY (2010) Decreasing pH trend estimated from 25-yr time series of carbonate parameters in the western North Pacific. *Tellus Ser B* 62:649–659
- Miyazawa Y, Zhang R, Guo X, Tamura H, Ambe D, Lee JS, Okuno A, Yoshinari H, Setou T, Komatsu K (2009) Water mass variability in the western North Pacific detected in a 15-year eddy resolving ocean reanalysis. *J Oceanogr* 65:737–756
- Nishikawa S, Tsujino H, Sakamoto K, Nakano H (2010) Effects of mesoscale eddies on subduction and distribution of Subtropical Mode Water in an eddy-resolving OGCM of the western North Pacific. *J Phys Oceanogr* 40:1748–1765
- Oka E (2009) Seasonal and interannual variation of North Pacific Subtropical Mode Water in 2003–2006. *J Oceanogr* 65:151–164
- Oka E, Qiu B (2012) Progress of North Pacific mode water research in the past decade. *J Oceanogr* 68:5–20
- Oka E, Suga T (2003) Formation region of North Pacific subtropical mode water in the late winter of 2003. *Geophys Res Lett* 30:2205. doi:10.1029/2003GL018581
- Oka E, Talley LD, Suga T (2007) Temporal variability of winter mixed layer in the mid- to high-latitude North Pacific. *J Oceanogr* 63:293–307
- Oka E, Suga T, Sukigara C, Toyama K, Shimada K, Yoshida J (2011) “Eddy-resolving” observation of the North Pacific Subtropical Mode Water. *J Phys Oceanogr* 41:666–681
- Oka E, Qiu B, Kouketsu S, Uehara K, Suga T (2012) Decadal seesaw of the Central and Subtropical Mode Water formation associated with the Kuroshio Extension variability. *J Oceanogr* 68:355–360
- Palter JB, Lozier MS, Barber RT (2005) The effect of advection on the nutrient reservoir in the North Atlantic subtropical gyre. *Nature* 437:687–692

- Qiu B, Chen S (2005) Variability of the Kuroshio Extension jet, recirculation gyre and mesoscale eddies on decadal timescales. *J Phys Oceanogr* 35:2090–2103
- Qiu B, Chen S (2006) Decadal variability in the formation of the North Pacific Subtropical Mode Water: oceanic versus atmospheric control. *J Phys Oceanogr* 36:1365–1380
- Qiu B, Chen S, Hacker P (2007) Effect of mesoscale eddies on Subtropical Mode Water variability from the Kuroshio Extension System Study (KESS). *J Phys Oceanogr* 37:982–1000
- Qiu B, Chen S, Schneider N, Taguchi B (2014) A coupled decadal prediction of the dynamic state of the Kuroshio Extension system. *J Clim* 27:1751–1764
- Rainville L, Jayne SR, McClean JL, Maltrud ME (2007) Formation of Subtropical Mode Water in a high-resolution ocean simulation of the Kuroshio Extension region. *Ocean Modell* 17:338–356
- Rainville L, Jayne SR, Cronin MF (2014) Variations of the North Pacific Subtropical Mode Water from direct observations. *J Clim* 27:2842–2860
- Roemmich D, Boebel O, Desaubies Y, Freeland H, King B, LeTraon PY, Molinari R, Owens WB, Riser S, Send U, Takeuchi K, Wijffels S (2001) Argo: The global array of profiling floats. In: Koblinsky CJ, Smith NR (eds) *Observing the oceans in the 21st century*. GODAE Project Office, Bureau of Meteorology, Melbourne, pp 248–258
- Sasaki YN, Minobe S (2015) Climatological mean features and interannual to decadal variability of ring formations in the Kuroshio Extension region. *J Oceanogr* (in press)
- Suga T, Hanawa K (1990) The mixed layer climatology in the northwestern part of the North Pacific subtropical gyre and the formation area of Subtropical Mode Water. *J Mar Res* 48:543–566
- Suga T, Hanawa K (1995a) The Subtropical Mode Water circulation in the North Pacific. *J Phys Oceanogr* 25:958–970
- Suga T, Hanawa K (1995b) Interannual variations of North Pacific Subtropical Mode Water in the 137°E section. *J Phys Oceanogr* 25:1012–1017
- Suga T, Hanawa K, Toba Y (1989) Subtropical Mode Water in the 137°E section. *J Phys Oceanogr* 19:1605–1618
- Suga T, Motoki K, Aoki Y, Macdonald AM (2004) The North Pacific climatology of winter mixed layer and mode waters. *J Phys Oceanogr* 34:3–22
- Suga T, Aoki Y, Saito H, Hanawa K (2008) Ventilation of the North Pacific subtropical pycnocline and mode water formation. *Prog Oceanogr* 77:285–297
- Sugimoto S, Hanawa K (2005) Remote reemergence areas of winter sea surface temperature anomalies in the North Pacific. *Geophys Res Lett* 32:L01606. doi:[10.1029/2004GL021410](https://doi.org/10.1029/2004GL021410)
- Sugimoto S, Hanawa K (2010) Impact of Aleutian Low activity on the STMW formation in the Kuroshio recirculation gyre region. *Geophys Res Lett* 37:L03606. doi:[10.1029/2009GL041795](https://doi.org/10.1029/2009GL041795)
- Takahashi T et al (2009) Climatological mean and decadal change in surface ocean pCO<sub>2</sub>, and net sea-air CO<sub>2</sub> flux over the global ocean. *Deep-Sea Res* 56:554–577
- Takatani Y, Sasano D, Nakano T, Midorikawa T, Ishii M (2012) Decrease of dissolved oxygen after the mid-1980s in the western North Pacific subtropical gyre along the 137°E repeat section. *Global Biogeochem Cycles* 26:GB2013. doi:[10.1029/2011GB004227](https://doi.org/10.1029/2011GB004227)
- Takikawa T, Ichikawa H, Ichikawa K, Kawae S (2005) Extraordinary subsurface mesoscale eddy detected in the southeast of Okinawa in February 2002. *Geophys Res Lett* 32:L17602. doi:[10.1029/2005GL023842](https://doi.org/10.1029/2005GL023842)
- Talley LD (1988) Potential vorticity distribution in the North Pacific. *J Phys Oceanogr* 18:89–106
- Uchida H, Kawano T, Kaneko I, Fukasawa M (2008) In situ calibration of optode-based oxygen sensors. *J Atmos Oceanic Technol* 25:2271–2281
- Xie SP, Xu LX, Liu Q, Kobashi F (2011) Dynamical role of mode-water ventilation in decadal variability in the central subtropical gyre of the North Pacific. *J Clim* 24:1212–1225
- Xu L, Xie SP, McClean JL, Liu Q, Sasaki H (2014) Mesoscale eddy effects on the subduction of North Pacific mode waters. *J Geophys Res*. doi:[10.1002/2014JC009861](https://doi.org/10.1002/2014JC009861)